ELSEVIER

Journal of Photochemistry and Photobiology A: Chemistry 125 (1999) 1–11

Journal of Photochemistry and Photobiology A:Chemistry

Real time study of the infrared multiphoton dissociation of vinylbromide

Bousselham Samoudi[a], Luis Díaz[a], Mohamed Oujja[b,*], Magna Santos[a]

[a]*Instituto de Estructura de la Materia, CSIC, Serrano 121, 28006 Madrid, Spain*
[b]*Instituto de Química-Fisica 'Roca Solano', CSIC, Serrano 119, 28006 Madrid, Spain*

Accepted 29 March 1999

Abstract

The infrared multiphoton dissociation of vinylbromide has been study in real time by the analysis of the spontaneous luminescence emitted in the dissociation process and by laser induced fluorescence of C_2 and CH species. It has been found that, although the dissociation of vinylbromide is a non-collisional process, formation of C_2 and CH takes place through a collisional process in the presence of the infrared laser field. Laser induced fluorescence excitation spectra of C_2 demonstrate that it is formed vibrationally hot in the ground state, its vibrational temperature estimated to be 2200 ± 200 K. The addition of Ar increases the dissociation yield of vinylbromide by a rotational hole filling effect but, for pressures higher than 12 hPa, the production of excited $C_2(d^3\Pi_g)$ is strongly quenched. These experiments have shown also that, in the ground state, approximately five times more population is formed vibrorotationally excited than in the $\nu'' = 0$ level, not depending on the fluence of the laser pulses. C_2H_2, HBr and H_2 are found as final products for fluences of 170 J/cm^2. For fluences of approximately 300 J/cm^2 diacetylene and a solid black soot are also formed.

1. Introduction

Multiple-photon dissociation of polyatomic molecules induced by intense infrared radiation (IRMPD) from a CO_2 laser has been employed frequently for obtaining free radicals and fragments of interest in kinetic studies [1]. Elementary reactions involving small carbon species like C_2 and C_3 play important role in the high temperature chemistry of hydrocarbons, as, for example, in the formation and decay of the recently discovered C_{60} fullerene [2,3]. C_2 is formed following IRMPD of a variety of polyatomic molecules [4–6], and among them, vinylhalides are systems that possess simple laser induced chemistry [7,8].

At present and up to our knowledge, no IRMPD of vinylbromide (VBr) has been reported, however thermal [9] and UV photolytic [10,11] decomposition of VBr in the gas phase have been studied. Multiple-photon absorption and dissociation under IR irradiation take place through different processes than UV multiphoton absorption or thermal decomposition. IRMPD proceed in the vibrational manifold of the electronic ground state usually by the minimum energy channel, but vibrational energies above the dissociation threshold can be reached transferring the energy excess to the dissociation products. Thermal decomposition takes place in the ground state by the minimum energy channel, although wall effects can become important in the decomposition process, effects that do not occur in IRMPD. On the other hand, in opposition to IRMPD, UV multiphoton dissociation takes place in an excited electronic state.

IRMPD of vinylchloride [8,12] and vinylfluoride [7,13] proceed via the lowest available channel, that is, the direct dehydrohalogenation. Thus the major products are acetylene and HCl or HF, respectively. Other products identified as diacetylene and solid soot are also found in the IRMPD of vinylchloride when it is irradiated at high fluence.

Following the research lines in our group [14,15], in this work we study the IRMPD of VBr through real time techniques, visible spontaneous luminescence (SL) and laser induced fluorescence (LIF). The obtained SL emission spectrum have been assigned to the Swan bands of the excited C_2 molecule ($d^3\Pi_g \rightarrow a^3\Pi_u$ transition) and to the CH fragment ($A^2\Delta \rightarrow X^2\Pi$ transition). We have observed that the formation of these species is due to the simultaneous interaction of collisions and infrared radiation on the initially formed excited precursor, probably acetylene. We have carried out LIF detection of the produced fragments obtaining that the population of C_2 formed in the ground state is vibrationally hot.

2. Experimental

A Lumonics K-103 TEA CO_2 laser is employed for the IRMPD of the VBr samples. It is equipped with a frontal Ge

*Corresponding author:

1010-6030/99/$ – see front matter
PII: S1010-6030(99)00078-7

multimode optics (35% reflection) and a rear diffraction grating with 135 lines/mm blazed at 10.6 μm. The irradiation is carried out using the 10P(24) line at 940.56 cm^{-1}, nearly coincident with the ν_5 torsion mode of VBr. The wavelength is checked with a 16-A spectrum analyser (Optical Eng. Co.). The laser operates with a mixture of CO_2, N_2 and He in the proportion 8 : 8 : 84, the pulse temporal profile being monitored with a photon drag detector (Rofin Sinar 7415). This temporal profile, at the above mentionedline, consists of a spike of 60 ns (FWHM) followed by a tail of approximately 3 μs long. Sometimes we have removed N_2 from the mixture to obtain a tail-free pulse of 60 ns (FWHM).

The photolysis experiments (Fig. 1) are performed under gasflow conditions in a Pyrex cell of 4.5 cm diameter and 25 cm length, fitted with a pair of NaCl windows orthogonal to another pair of quartz windows. The CO_2 laser beam is focused at the centre of this reaction cell by a NaCI lens of 24 cm focal length. In some experiments tight focused irradiation was used employing a 5 cm focal length lens and a 10 cm long cell. Analysis of the final stable products is carried out by FTIR spectroscopy.

Fluorescence is induced in the formed fragments by means of a N_2-pumped dye laser (PRA LN1O7) with a bandwith of 1.6 cm^{-1} at 500 nm. The beam, counter-propagating to the CO_2 laser beam, is focused by a 50 cm quartz lens at the focus of the infrared beam. The relative energy of the dye laser was controlled with a Thorlabs high speed silicon detector.

SL and induced fluorescence are detected through a quartz window at right angle to the laser axis after focusing onto a P28 RCA photomultiplier tube through interference filters centred at 560, 488 and 431 nm (10 nm FWHM in all the cases) for $C_2(0,1)$, CH(0,1) and CH(0,0) transitions respectively. To obtain the SL spectrum the signal was dispersed with a Bausch and Lomb 10 cm monocromator with 2 mm slits that was used as filter (15 nm resolution).

The CO_2 laser pulse, picked up with the photon drag detector, triggers a Tektronix TDS 540 digital oscilloscope that is used to collect the signals and send them to a personal computer where they are averaged and analysed. The delay between the CO_2 laser and the probe laser is controlled by a Berkeley Nucleonic BNC 7036A to within ∼50 ns. The CO_2 laser fluence is calculated as the ratio of the pulse energy, as measured with a Lumonics 20D pyroelectric detector, and the FWHM cross-sectional beam area, measured at the cell position with a pyroelectric array Delta Development Mark IV. The obtained fluence with the 24 cm focal length lens is 170 J/cm^2 for the tailed pulses and 50 J/cm^2 for the tail-less pulses. With the 5 cm focal length lens the fluence is higher than 300 J/cm^2 for tailed pulses. All the experiments, if it is not indicated, have been done with the 24 cm lens.

Each point is obtained by averaging over 20 measurements. In the average, each signal is shifted to a common time origin defined by the CO_2 laser in SL measurements or by the probe pulse in LIF. LIF signals are normalised for energy variations of the probe laser beam. The intensity of the LIF signal at each experimental condition is calculated by integration in a temporal window from 12 to 400 ns. The total signal in SL experiments was integrated.

The sample pressure in the gas flow cell is measured with a 0–10 hPa MIKS Baratron gauge being the rate of the CO_2 pulse so that a new fresh sample is irradiated in each shot. The VBr samples have been purchased from Merck (99.0%) and degassed prior to use.

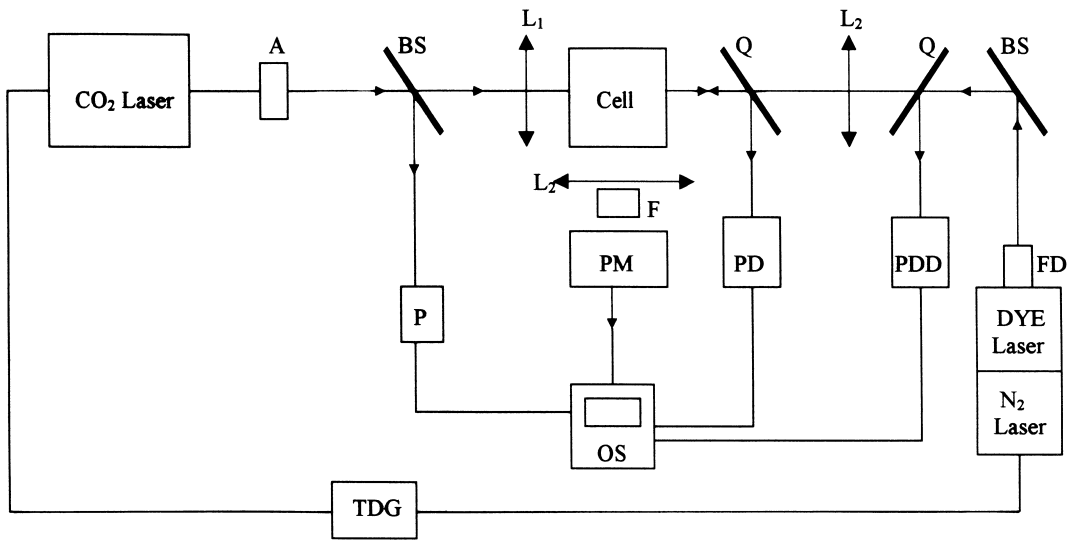

Fig. 1. Experimental set-up. A: attenuators; BS: beam-splitter; F: filter/monocromator; FD: frequency doubler; L_1: NaCl lens; L_2: quartz lens; OS: oscilloscope; P: pyroelectric detector; PD: photon drag detector; PDD: photodiode detector; Q: quartz plate; PM: photomultiplier; TDG: trigger and delay generator.

3. Results and discussion

IRMPD of VBr using the 10P(24) line of a TEA CO_2 laser produces C_2H_2, HBr and a non-condensable gas, assumed to be hydrogen as final stable products. Additional production of C_4H_2 and a black carbon soot was found when a tight focussed beam (5 cm focal length lens) was used. No solid products were found with the 24 cm lens in any experiment, even if a NaCI substrate was introduced in the cell and analysed by FTIR spectroscopy after irradiation of 10 hPa of VBr with more than 600 shots.

3.1. Spontaneous luminescence

Irradiation of VBr gives rise to a spontaneous visible luminescence emission in the pressure range studied (0.5–15 hPa) for tailed and tail-free pulses. No luminescence was detected when VBr was irradiated with the non resonant 10R(24) (978.49 cm^{-1}) line, indicating that the dissociation of VBr takes place through a resonant absorption process, at least at the fluences used in this work.

The visible luminescence signal was dispersed in the 320–600 nm range obtaining the spectrum shown in Fig. 2. This spectrum consists of several vibronic bands without rotational resolution, superimposed to a broad background. This pattern is usual in the SL spectra in IRMPD experiments [16–18] and the background has been explained as due to the emission of molecular fragments larger than diatomic [19] or to the blackbody radiation spectrum [20]. We assign the obtained bands at 436, 472, 514 and 560 nm to the emissions from the $C_2(d^3\Pi_g - a^3\Pi_u)$ $\Delta\nu = 2, 1, 0$ and -1 Swan bands and those at 430, 486 nm to the emissions from the $CH(A^2\Delta - X^2\Pi)$ $\Delta\nu = 0$ and -1 transitions.

Irradiation of VBr with tailed laser pulses produces a luminescence signal with a temporal profile different from that obtained when tail-free laser pulses are used. Fig. 3 shows the temporal profiles of the luminescence signals filtered at the $\Delta\nu = -1$ transition of the C_2 Swan bands for the irradiation of several initial pressures of VBr: (a) with a tailed pulse and (b) with a tail-free pulse. The temporal profiles of the respective CO_2 laser pulses are also shown. Luminescence signals arising from irradiation of VBr with

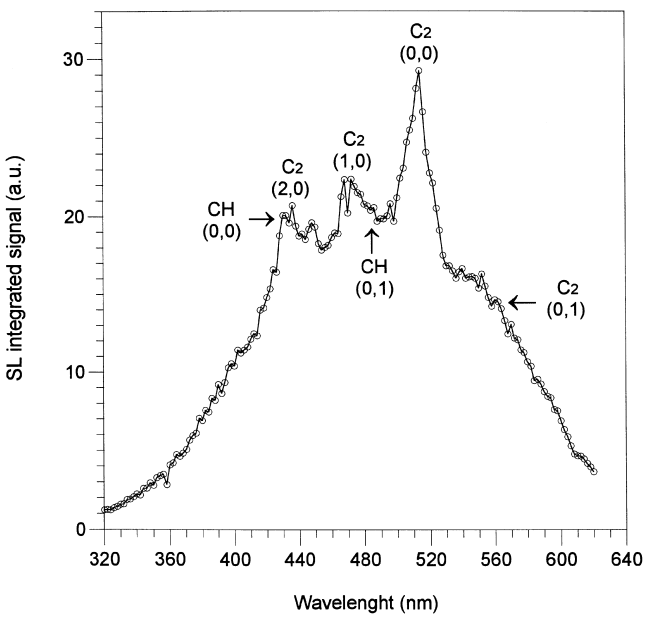

Fig. 2. Emission spectrum of the SL resulting from the IRMPD of 4 hPa of VBr taken with a resolution of 15 nm. The C_2 and CH assigned bands are indicated.

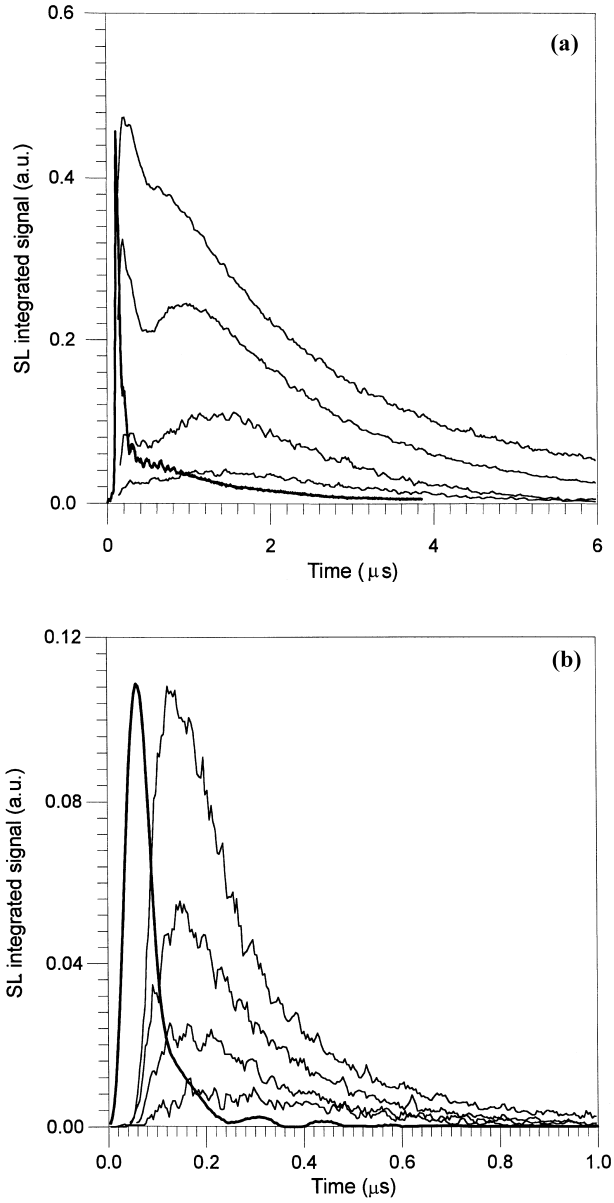

Fig. 3. Temporal profiles of the SL from the $C_2(d^3\Pi_g - a^3\Pi_u)$ $\Delta\nu = -1$ transition for the irradiation of (a) 1, 2, 10 and 17 hPa of VBr with tailed pulses and (b) 1.5, 3, 4 and 6 hPa of VBr with tail-free pulses. The temporal profiles of the respective CO_2 laser pulses are also shown with bold trace.

tailed pulses consist of an initial maximum followed by another broad one. The first maximum, that appears at pressures higher than 1.3 hPa, always peaks 80 ns after the CO_2 maximum (160 ns after the onset of the laser pulse), conditions at which no single collision between VBr molecules takes place; its rise always follows the CO_2 pulse, indicating that radical production is driven by the temporal profile of the CO_2 laser pulse. The second maximum consists of a broad signal that reaches the maximum at a time at which more than two collisions between VBr molecules have taken place. The time between the two maxima decreases linearly with the pressure. Tail-free pulse irradiation produces a luminescence signal which consists of a unique maximum that peaks around 70 ns and also follows the rise of the CO_2 tail-free pulse for all the studied pressure interval. Temporal profiles of the luminescence signals filtered at the $\Delta\nu = 0$ transition of CH mimic the C_2 luminescence signals for tailed and tail-free pulses. Such temporal profiles of SL are characteristic of all the luminescence signals detected along the whole spectrum of Fig. 2. In addition, we have compared the luminescence spectra gating the signal at each of the two maxima obtained with tailed pulses, and no difference have been found. This result rules out the possibility of two different emission processes at two different times.

The dependence of the luminescence signal on the VBr pressure that is implicit in Fig. 3 is apparent in Fig. 4 where the integrated signal versus pressure is plotted. The variation of the luminescence is linear with pressure and shows two different pressure thresholds for both kinds of CO_2 pulses but the same for both, C_2 and CH. For tailed pulses a threshold of 0.25 hPa is found from the linear fit of the experimental points of Fig. 4. In the 0.25–1.3 hPa interval only the broad signal is detected which reaches its maximum in the time of the tailed pulse; for higher pressures the initial luminescence maximum appears. For tail-free pulses the pressure threshold is reached at a pressure of 1.1 hPa, higher than the one found for tailed pulses as it is expected due to the lower fluence of those pulses.

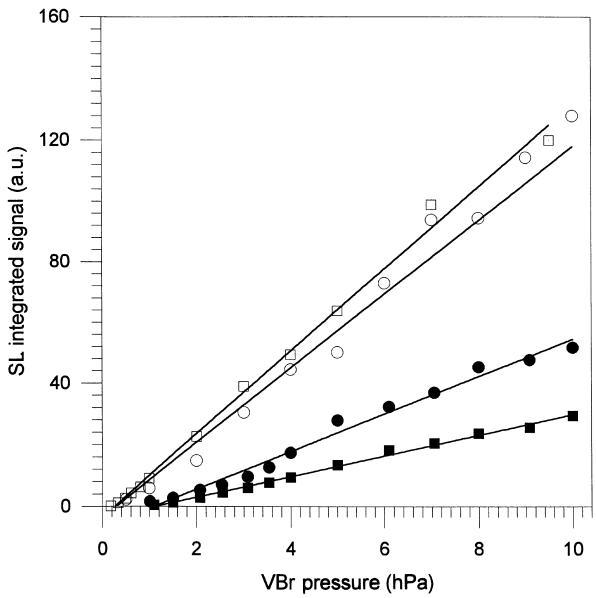

Fig. 4. Integrated signal of the SL vs. vinylbromide pressure. The irradiation was carried out with tailed CO_2 pulses (open symbols) and with tail-free CO_2 pulses (full symbols). The emissions correspond to: ● the $C_2(d^3\Pi_g - a^3\Pi_u)$ $\Delta\nu = -1$ transition; ○ the $C_2(d^3\Pi_g - a^3\Pi_u)$ $\Delta\nu = -1$ transition; ■ the $CH(A^2\Delta - X^2\Pi)$ $\Delta\nu = -1$ and □ the $CH(A^2\Delta - X^2\Pi)$ $\Delta\nu = 0$.

The obtained dependence of the luminescence on pressure indicates that the production of the excited C_2 and CH species arises from a collisional assisted process. Since both signal maxima occur within the CO_2 laser pulse and production does not occur after the pulse, collisions taking place without the presence of laser pulse are not responsible for the formation of such fragments. As mentioned above, the initial maximum for C_2 or CH appears always 160 ns after the onset of CO_2 pulse, time that is smaller than the time for one collision between VBr molecules to take place at the threshold pressure for this maximum (185 ns). These data suggest that the dissociation of VBr takes place through a non-collisional process and that collisions in the time of pulse between vibrational excited products are responsible for the production of C_2 and CH. Thus, for tailed pulses and for low pressures, excited products absorbing from the tail of the laser pulse and colliding produce excited C_2 and CH giving rise to the delayed broad maximum at a time determined by the parent pressure. Increasing the pressure, the initial maximum appears, driven by the CO_2 pulse, at the minimum time necessary for the collisional assisted excitation process of the resulting products. C_2 production through different secondary processes has been reported. Li and Francisco [6] found by LIF in the IRMPD of *bis*-trifluomethyl peroxide that C_2 is not a primary photofragment but it is produced within the laser pulse from secondary IRMPD of photofragments, without the assistance of collisions. Yu et al. [21] have found by LIF the C_2 radical in the collision-free IRMPD of C_2H_3CN as secondary photofragment. Lesiecki and Guillory [22] found by SL that collisional processes, subsequent to the laser pulse, are effective in producing C_2. In our case both collisions and absorption of IR photons are necessary simultaneously.

Similar temporal profiles have been found in IRMPD of 1,2-dibromo-1,1-difluoroethane [17] and 1,2-dichloro-1,1-difluoroethane [18]. However, two maxima are obtained in all the studied pressure interval ($\geq$1 hPa). The authors attribute the luminescence emission to the formation of transient carbenes as primary photofragment; the first maximum arises during the spike of the laser pulse and the hot undissociated molecules are subsequently excited and dissociated in a collisional assisted process by the pulse tail giving rise to the second one.

The addition of inert buffer gas produce collisional effects in the absorption–dissociation process related to rotational and vibrational relaxation processes. In rather small molecules with a low dissociation yield, rotational relaxation is a cooperative effect by means of which the rotational bottle-

neck may be overcome by rotational hole filling (RHF) [23] allowing a larger amount of energy to be absorbed. The vibrational quenching that opposes to the energy absorption by relaxing the excited vibrational levels, is usually much slower than the pumping rate, so such relaxation is efficient in times larger than IR pulses. However if sufficient buffer gas is added, vibrational relaxation can occur in the time of the pulse, as is characteristic of highly excited molecules [24], decreasing the dissociation yield [8]. In the IRMPD of vinylchloride the addition of less than 1 Torr of He to 1 Torr of vinylchloride induces a drop of 50% on the dissociation yield [8] due to the fact that the buffer gas removes a substantial amount of vibrational energy from the molecule by efficient V-T processes. In the case of vinylfluoride, 10 Torr of several buffer gases (He, Ar, N_2, Xe and H_2) added to 50 mTorr of vinylfluoride produce an enhancement of more than three times in the IR luminescence signal emitted by vibrational excited HF; for higher buffer pressures a slight decrease was found [7,13]. The enhancement was explained by RHF. In our case, for a fixed amount of VBr (0.5 or 0.16 hPa), addition of several Ar pressures induces in the C_2 production both, an initial increase for Ar pressures until 12 hPa and, for higher buffer pressures, a strong decrease as can be seen in Fig. 5. This last effect is also shown in the insert of Fig. 5 where the luminescence signals for 12 and 80 hPa of Ar added to 0.5 hPa of VBr are plotted. As can be seen, high Ar pressures give rise to a strong quenching of C_2 luminescence. This effect may be a consequence of a very efficient vibrational relaxation of the excited precursors of C_2 inhibiting its production. For low Ar pressures contribution of rotational hole filling becomes dominant. The rotational hole filling effect induced by Ar produces different efficiency for different pressures of VBr. Thus an increase of dissociation of 2.5 and 6 is obtained for 0.5 and 0.16 hPa of VBr, respectively. This effect could be explained considering that, for high pressures, homogeneous collisions help to overcome the vibrational bottleneck, decreasing the number of excited VBr molecules able to interact with Ar, resulting in a decreasing of the rotational hole filling effect.

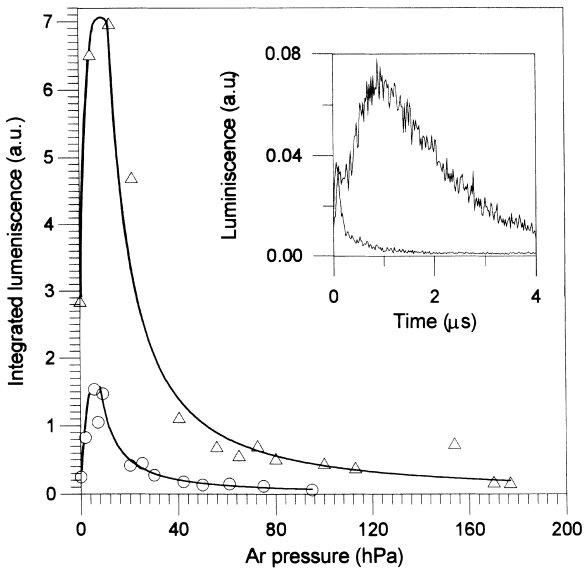

Fig. 5. Integrated signal of the SL vs. Ar pressure for vinylbromide pressures of: ○ 0.16 hPa and △ 0.5 hPa. In the insert are plotted the temporal profiles of the signals corresponding to 80 hPa (lower trace) and 12 hPa (upper trace) of Ar.

When different VBr pressures were irradiated with tailed pulses in the 0.14–0.8 hPa interval, keeping constant the Ar pressure (20 hPa), a linear dependence of the luminescence signal on VBr pressure was found. However due to the RHF effect cited above, the pressure threshold for luminescence decreases until 0.04 hPa and the pressure at which the first maximum appears lowers to 0.2 hPa with respect to pure VBr experiments. On the other hand, the time at which the luminescence reaches the initial maximum is, when it appears, always 60 ns later than in pure VBr (i.e. 220 ns after the onset of CO_2 pulse). This increase in the minimum time necessary to reach the first maximum in the C_2 production in presence of Ar may be related with the time necessary for the RHF effect to take place.

Analysis of the luminescence decay versus pressure have been performed in the tail-free experiments where a least-squared line fitting to single exponential function is possible. From the Stern–Volmer plots of the decay rates of the $C_2(d^3\Pi_g)$ and $CH(A^2\Delta)$ radiative lifetimes of 335 ± 20 ns for C_2 and of 780 ± 20 ns for CH are calculated. These lifetimes are longer than the radiative lifetimes of the respective electronics states, since production rates of $C_2(d^3\Pi_g)$ and $CH(A^2\Delta)$ are driven by the time width of the laser pulse and dominate the emission process as has been found in other emissions from IRMPD [18]. The different lifetimes values obtained for C_2 and CH sustain the assignment given in the SL spectrum for the transitions of these two species.

3.2. Laser induced fluorescence

Using the suitable dye we have scanned the dye laser in different spectral regions, following 800 ns the infrared irradiation of 0.5 hPa of pure VBr. We have obtained the excitation spectra of C_2 shown in Fig. 6 where the increment in the excitation scan is 0.1 nm, and the $\Delta\nu = -1$ emission sequence of the Swan band have been monitored. In the spectral interval between 468 and 520 nm, it can be observed that, besides the bandheads corresponding to the (0,0) and (1,0) transitions, those corresponding to the (1,1) and (2,1) transitions are also observed. In addition, some spiky rotational structure corresponding to the R branch of the $\nu'' = 0$ level can be identified. The much lower intense (2,0) transition is shown in the interval 436–438 nm.

The appearance of the (1,1) and (2,1) bandheads denotes that a rather high proportion of C_2 fragments are formed in the $\nu'' = 1$ vibrational levels, and therefore vibrationally hot. Other authors who have obtained C_2 from the unimolecular

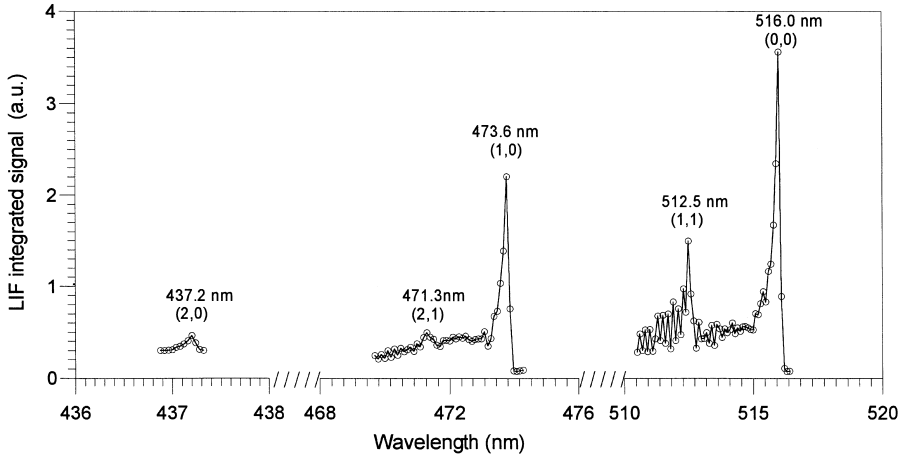

Fig. 6. LIF excitation spectra of the Swan bands of C_2 following the IRMPD of 0.5 hPa of neat VBr.

IRMPD of different parent molecules have not detected LIF signals from levels other than $\nu'' = 0$ [21,25]. This suggests that the collisional character of the C_2 production from the IRMPD of VBr, may be responsible for the hotter vibrational temperature, as was proven in the IRMPD of C_2H_4 [26]. From the values of the integrated areas of the bands in Fig. 6 and the Franck–Condon factors given in the literature [27], assuming a Boltzmann distribution, we have estimated an effective vibrational temperature for the formed C_2 of 2200 ± 200 K. This value is higher than the vibrational temperature obtained for C_2 from IRMPD of ethylene at higher values of pressure [26], where for 1.3 hPa of C_2H_4 a vibrational temperature of 1400 K was obtained. In the dissociation of VBr other products than the C_2 precursor are formed, so that the effective collisional rate is higher in IRMPD of VBr for the same initial concentration.

Fig. 7(a) shows the variation with pressure of the LIF signal originated by exciting at 515.5 nm the (0,0) transition of the C_2 species produced via IRMPD of VBr for different time delays between CO_2 and dye lasers. Although a linear relationship is obtained up to initial concentrations of 1 hPa, the intercept at $\sim$0.15 hPa indicates that no C_2 could be detected at pressure lower that this limit, confirming the collisional production observed in the experiments of SL. This threshold is lower than that obtained from the SL as could be expected from the much more sensitivity of the LIF technique and also by considering that both signals come from different excited levels of C_2, more energetic and probably with less population in the case of the electronic excited levels detected by SL. The decrease in the line slopes obtained as the time delay increases indicates that the concentration of the C_2 species in the probed

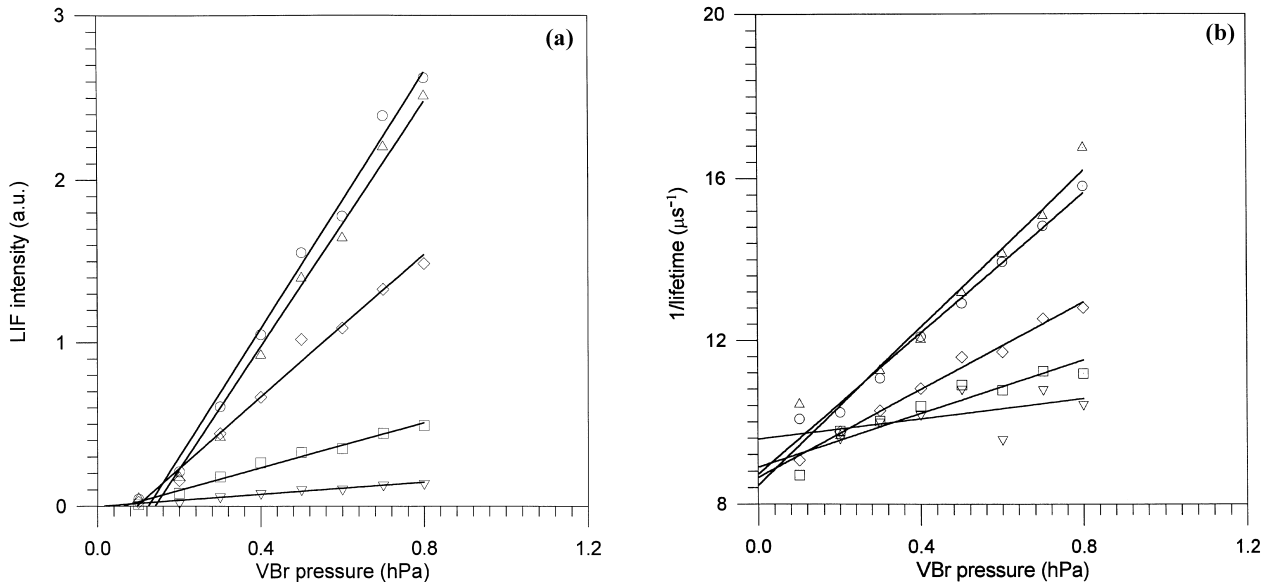

Fig. 7. (a) C_2 LIF integrated signal vs. VBr pressure at several delays from the photolysis laser. (b) Decay rates of the LIF signals. Δ 400 ns; $\bigcirc$ 800 ns; $\Diamond$ 1 μs; $\square$ 4 μs and ∇ 8 μs.

zone is becoming smaller as the time for the probe is increased.

We have been able to carry out least-squared line fitting of the LIF signals to single exponential functions after the subtraction of a small background arising from the spontaneous emission and truncation to avoid initial perturbation by the production laser spike and residual noise at low signal intensity. The pressure dependencies of the $C_2(d^3\Pi_g, \nu' = 0)$ fluorescence decay rates are given on Fig. 7(b) for each of the time delays studied. We have plotted also the lifetime values of the LIF signals obtained for the dissociation of several initial concentrations of VBr probed at different time delays from the CO_2 laser (Fig. 8). As it can be seen, for the two higher VBr initial concentrations, the lifetime values increase with the time delay.

The behaviours obtained for the lifetimes of the excited state $C_2(d^3\Pi_g)$ and for the decay rates of this state by VBr molecules and dissociation products is not very strange if one takes into account the dense cloud of products in the reaction zone that diffuse out from it allowing a smaller quenching of the signal as the probe is delayed. To obtain significant values for these two parameters it would be necessary to carry out the experiments at times with delays above 6 μs. Nevertheless, the large rate of disappearance the C_2 species that we have checked (see later) prevent these type of experiments. However, from the lines of Fig. 7(a and b) an upper limit of 104 ns for the non-collisional lifetime of the $C_2(d^3\Pi_g)$ is obtained. This value is in accordance with the lifetime value given in the literature for this state [28,29]. An upper limit for the quenching rate constant for this state with VBr molecules and dissociation products of 5.0×10^{-11} s^{-1} molecules^{-1} cm^3 is obtained.

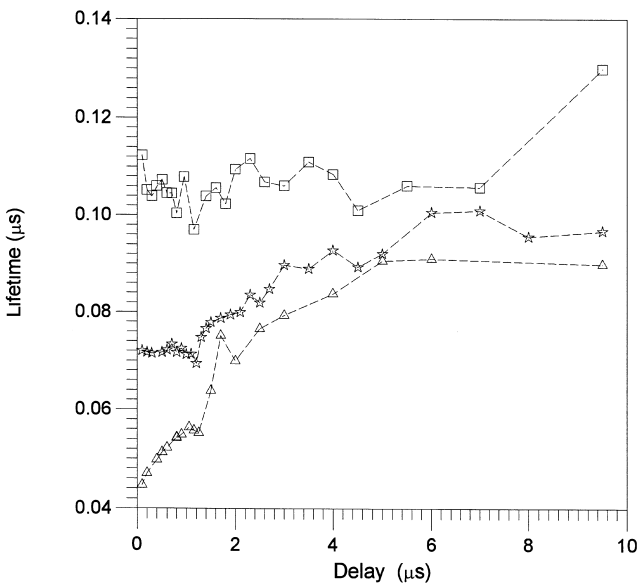

Fig. 8. Collisional lifetimes of the C_2 LIF signals vs. the time delay between the photolysis and probe pulses, for several initial VBr concentrations. □ 0.16 hPa; ☆ 0.5 hPa; Δ 1.0 hPa.

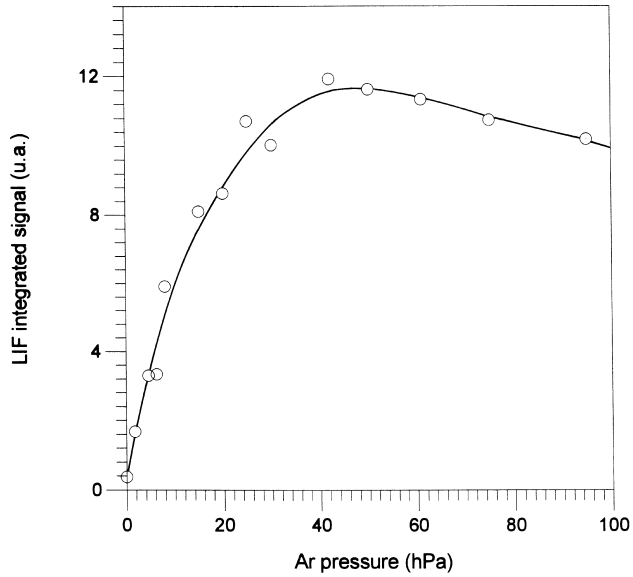

Fig. 9. C_2 LIF integrated signal vs. the pressure of Ar added to 0.16 hPa of VBr

Fig. 9 shows the LIF intensity of the signal for the produced $C_2(a^3\Pi_u, \nu'' = 0)$ when the dissociation of 0.16 hPa of VBr is carried out in the presence of increasing quantities of Ar. As it can be seen, the addition of Ar up to 44 hPa significantly increases the amount of the detected C_2 signal. This increase is as high as 29 times for the smallest initial VBr studied pressure. From this value of Ar, the induced fluorescence signal decreases. As it is well known, the addition of an inert buffer gas enhances the C_2 detection by controlling the diffusion processes and inducing its vibrorotational relaxation. At 800 ns from the photolysis laser and at the VBr pressure used, the diffusion of C_2 out of the volume being probed is quite small [13], scarcely contributing to the total increase. The SL signal recorded when the dissociation of VBr is carried out in the presence of Ar (Fig. 5) indicates that there is an increase in the amount of C_2 excited to the upper electronic states that is up to a factor of 6 for the smallest VBr pressure studied. We have assigned this increase to the existence of an effect of RHF in the unimolecular dissociation of VBr. We assign then the high increase observed in the LIF detection of $C_2(a^3\Pi_u, \nu'' = 0)$ from the IRMPD of VBr in the presence of Ar as due to an actual increase in the formation of C_2 due to RHF in the dissociation of VBr, plus a large contribution from the relaxation of the initially formed rotational and vibrationally excited C_2. We have observed that up to the smallest VBr/Ar studied concentration (∼1/600) no quenching of the $C_2(d^3\Pi_g, \nu' = 0)$ state has been detected, as has been already pointed out by other authors for smaller Ar concentration [30,31]. This result together with the different increase of the LIF and SL signals detected when Ar is added, suggest that in the ground state approximately five times more population is formed vibrorotationally excited than in the $\nu'' = 0$ level. The shift in the position of the maximum in Fig. 9(a)

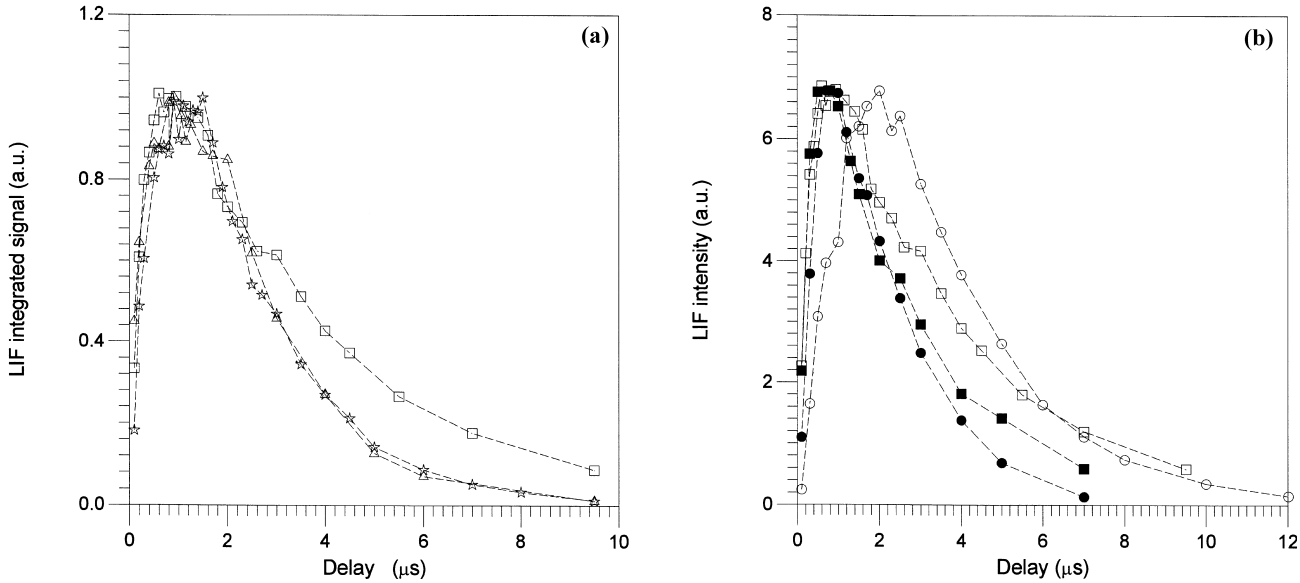

Fig. 10. Normalised C_2 LIF integrated signal vs. the time delay between the photolysis and probe pulses: (a) at several pressures of neat VBr: □ 0.16 hPa; ☆ 0.5 hPa; Δ 1.0 hPa, and (b) at the following conditions: □ 0.16 hPa (26); ○ 0.16 hPa + 20 hPa Ar; ■ 0.16 hPa, tail-free pulse (410); ● 0.16 hPa + 20 hPa Ar, tail-free pulse (16); the number in parenthesis are the normalisation factor with respect to the curve with 2113Ar (○).

with respect to the position of the maximum obtained in the equivalent experiments for the spontaneous emission may be due to the larger Ar pressure interval at which vibrorotational relaxation in the ground state takes place with respect to the interval for RHF. It could be also, that at large concentration of Ar, there is still formation of ground state C_2 but no electronically excited C_2.

Fig. 10(a) gives the normalised intensity of the LIF signal for $C_2(a^3\Pi_u, \nu'' = 0)$ produced when the time delay between the photolysis and probe laser is varied, for three different values of the initial concentration of VBr. The risetime of the curves are rather independent of the initial parent concentration in the studied interval. Although the decay time is driven by the spontaneous diffusion of the radicals out of the volume being probed by the excitation pulse, it is clear that the species decay rapidly. So, 10 μs after the CO_2 laser pulse there is no signal at 0.87 or 0.45 hPa. At 0.083 hPa there is still a small signal at this time, showing the collisional character of the disappearance of the C_2 species. The broad maxima obtained for the three pressure values can be understood as due to the collisional formation of C_2 from the dissociation product during the time of the tailed CO_2 pulse as well as to the relaxation of vibrorotationally excited C_2 back to the probed vibrational ground state.

Fig. 10(b) gives the normalised intensity of the LIF signal emitted by the C_2 from 0.16 hPa of pure VBr when the time delay between the photolysis and probe laser is varied compared to that obtained when the dissociation is carried out in the presence of 20 hPa of Ar. Experiments carried out with tail-free pulses at the same parent and buffer pressures are also shown. For comparison, the normalisation factors relative to the curve for tailed pulses in the presence of Ar are given. For the pulse with tail, the position of the maximum of the curve obtained in the presence of Ar is delayed 1.4 μs with respect to that obtained in the absence of the buffer gas indicating that, at these conditions, a large proportion of C_2 is formed in the tail of the pulse both, in the ground state and rotovibrationally excited, continuously decaying to the probed state. In the case of the pulses without tail the delay is 200 ns, related to the time for the formed vibrational and rotational excited molecules to relax to the probed ground $\nu'' = 0$ level. The maximum LIF intensity reached in the curve obtained in the presence of Ar for the pulse with tail is 26 times the maximum reached for the same kind of pulses in the case of neat VBr; the same factor as comparing the curves obtained for tail-free pulses, with and without Ar. Similar effect is obtained for the maximum of the curve for neat VBr and pulse with tail that is 16 times the maximum obtained for tail-free pulse, the same factor as comparing the experiments obtained with pulses with and without tail in the presence of Ar. In other words, for 0.16 hPa of VBr, the tail of the pulse increases the production 16 times and the presence of 20 hPa of Ar increases the population of the (0,0) state 26 times. Considering the temporal profiles and the energies of the pulses with and without tail one can consider that it is the fluence the more characteristic parameter for these two types of pulses with respect to the dissociation process. Taking into account that Ar induces rotovibrational relaxation in the $C_2(a^3\Pi_u)$ state, the obtained results suggest that, at the used experimental conditions, the fluence do not change the proportion of $C_2(a^3\Pi_u)$ produced in the $\nu'' = 0$ level with respect to the $C_2(a^3\Pi_u)$ rotovibrationally excited. Comparing the decay rates of the different curves, it can be observed that the decay rates are larger when Ar is present. This may be due to the collisional disappearance of the C_2 species that

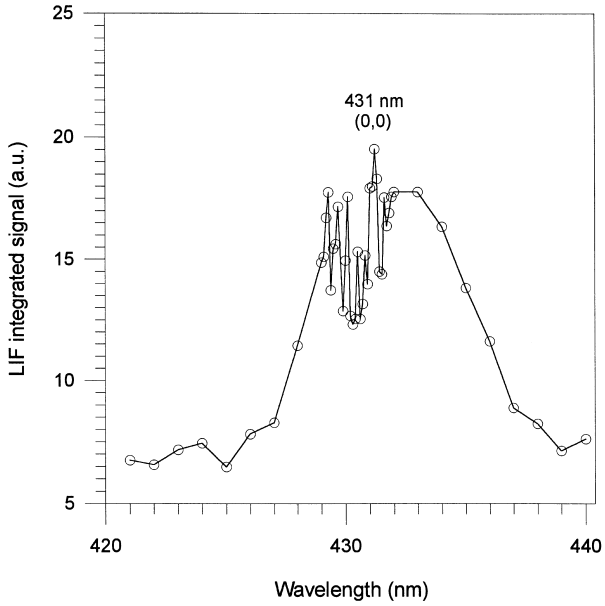

Fig. 11. LIF excitation spectrum of CH following 8 μs the irradiation of 5 hPa of neat VBr.

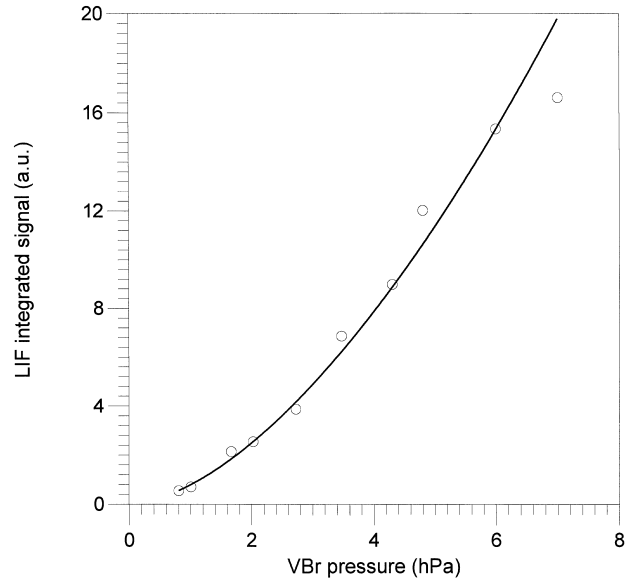

Fig. 12. CH LIF integrated signal vs. VBr pressure, at 8 μs time delay from the photolysis laser.

is favoured by the presence of the buffer, inhibiting the expansion of the collisional partners. These results confirm the low contribution to the LIF signal obtained in the presence of Ar that the diffusion process has.

To confirm the presence of CH among the dissociation products that has been assigned in the SL spectrum, we have carried out LIF experiments filtering the fluorescence signal at 488 nm. When the probe dye laser is less than 6 μs apart from the photolysis laser the LIF signal is very weak and superimposed to a strong SL signal. Scanning the dye laser 8 μs apart from the CO_2 laser we have obtained the fluorescence excitation spectrum of Fig. 11. A broad band with some rotational structure centred at 431 nm is obtained, corresponding to the ($A^2\Delta \rightarrow X^2\Pi$, $\Delta\nu = 0$) transitions of CH [32]. Some spiky structure corresponding to the Q branch of this band is also observed.

Studying the change of the LIF intensity when the time delay between the photolysis and the probe laser is varied, we obtain that the CH LIF signal remains up to more than 90 μs, showing that the time of permanence for this species is much longer than in the case of C_2. The overlap of the LW and SL signals that occurs before 6 μs could suggest that, different to the C_2 fragment, the CH species is mostly formed electronically excited. However, the big background obtained in the SL spectrum make doubtful this result.

The relation between the LIF signal emitted by the CH at 8 μs from the CO_2 laser and the VBr initial concentration is given in Fig. 12. The collisional character of the CH formation is clearly deduced from the larger than the one obtained with dependence between both the parameters. Single exponential fitting of the decay profiles of the LIF signals allows to obtain an upper limit for the non-collisional lifetime of 492 ns and a quenching rate for CH with VBr and dissociation products for the $\nu' = 0$ level of 5.93×10^{-10} s^{-1} $molecules^{-1}$ cm^3.

The results obtained from SL, from LIF as well as the analysis of the final products, suggest the following dissociation scheme:

$$H_2C = CHBr \xrightarrow{nh\nu} HBr^* + HC \equiv CH^* \quad (1)$$

$$HC \equiv CH^* + HC \equiv CH^* \xrightarrow{nh\nu} C_2(d) + C_2(a)^* + H_2 \quad (2)$$

$$HC \equiv CH^* + HC \equiv CH^* \xrightarrow{nh\nu} CH(A) + CH(X)^* \quad (3)$$

$$HC \equiv CH^* + HC \equiv CH^* \xrightarrow{nh\nu} H_2 + HC \equiv C - C \equiv CH \quad (4a)$$

$$H_2C = C : + HC \equiv CH^* \xrightarrow{nh\nu} H_2 + HC \equiv C - C \equiv CH \quad (4b)$$

Reaction (1) shows that IRMPD of VBr takes place by a non-collisional process as has been discussed in relation with both the temporal profile of the SL and the results in the presence of Ar. Dissociation of VBr proceeds via molecular elimination of HBr followed by rearrangement of vinylidene radical. Dehydrohalogenation was also found in the IRMPD of vinylfluoride [7,13] and vinylchloride [8,12] as the lowest available channel. Production of C_2H_2 and HBr also agree with theoretical studies of VBr decomposition on the ground-state potential energy surface [33–35]. These studies show that for excitation energies close to the energy required for VBr decomposition (3.105 eV) [33] the HBr yield is higher than 92.5%. Taking into account that IRMPD usually proceeds by the minimum energy channel, dehydrohalogenation should be the dominant channel in the IRMPD of

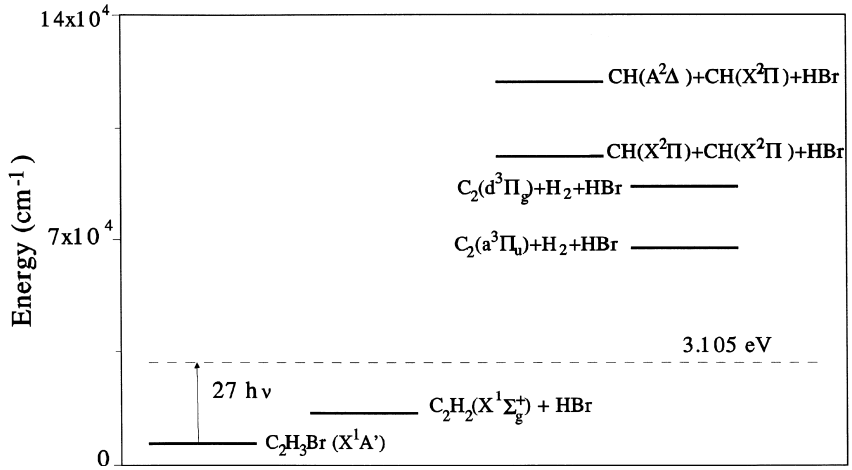

Fig. 13. Energy diagram for the formation of the excited C_2 and CH species from the IRMPD of the vinylbromide.

VBr. Other possible channel at excitation energy close to the dissociation threshold could be the Br elimination that has only been found in the 193 nm photolysis [10] occurring in the excited electronic state of VBr [36] that is not probable in IRMPD which takes place in the ground electronic state.

Our results indicate that $C_2(d^3\Pi_g)$ and $CH(A^2\Delta)$ arise in a collisional assisted processes between the products of the initial dissociation of VBr in the time of the pulse. The product more probably producing C_2, and CH is C_2H_2 that must be highly vibrational excited, possibly in the quasi-continuum, to be able to absorb IR radiation. In Fig. 13 the energy level diagram for the production of C_2 and CH from VBr is shown. Collisional assisted dissociation of acetylene, reaction (2), could yield $C_2(d^3\Pi_g)$ by two possible channels, a molecular elimination of H_2 or elimination of two hydrogen atoms via the C_2H intermediate. The H atom elimination channel needs an energy of 38 986 cm−1 (38 IR photons) more than the molecular elimination, so that reaction (2) seems to be the most probable channel to produce C_2 in the $d^3\Pi_g$ electronic state. Secondary collisional dissociation of acetylene, reaction (3), is also the most probable channel for $CH(A^2\Delta)$ production. Other possible channels involving C_2H and C_2H_3 as intermediates are not favourable energetically.

Formation of diacetylene, that has been found in tight focussed geometry, may be a secondary process from the excited C_2H_2 after initial dissociation of VBr, reaction (4a), or could be formed via vinylidene as intermediate for dimerization of acetylene [37], reaction (4b). In this irradiation condition production of black carbon soot may be initiated by the reaction of vinylidene with acetylene as has been suggested in [37].

4. Conclusions

We have studied in real time the IRMPD of VBr through the analysis of the spontaneously produced visible luminescence signal and inducing laser fluorescence in the C_2 and CH species formed in the dissociation process.

We have established that the dissociation of VBr takes place through a non-collisional process and that the fragments C_2 and CH are formed by a collisional process in the presence of infrared laser radiation from a previously produced precursor, probably vibrationally excited acetylene.

The C_2 and CH species are produced in the ground state and electronically excited. We have found that the population formed in the ground state is vibrationally hot, estimating the vibrational temperature in 2200 ± 200 K.

We have also shown that the presence of up to 12 hPa of Ar increase the VBr dissociation yield by a rotational hole filling effect. From this concentration of buffer the formation of electronically excited C_2 is quenched.

Finally, it has been observed that the fluence of the infrared laser beam do not change the proportion of $C_2(a^3\Pi_g)$ produced in the $\nu'' = 0$ level with respect to the $C_2(a^3\Pi_g)$ rotovibrationally excited, and that when Ar is added to 0.16 hPa of VBr approximately five times more population is formed vibrorotationally excited than in the $\nu'' = 0$ level.

Acknowledgements

The authors wish to acknowledge Dr. J.A. Torresano, Dr. M. Castillejo and Dr. M. Martin for useful discussions. This work was carried out with financial support provided by the Spanish DGES under Project number PB96-0844-C02-02.

References

[1] D.W. Lupo, M. Quack, Chem Rev. 87 (1987) 181.
[2] S.C. O'Brien, J.R. Heath, R.F. Curl, R.E. Smalley, J. Chem. Phys. (1998) 220.
[3] M. Ehbrecht, M. Faerber, F. Rohmund, V.V. Sminov, O. Stelmakh, F. Huisken, Chem. Phys. Lett. 214 (1993) 34.

[4] J.D. Campbell, M.H. Yu, C. Wittig, Appl. Phys. Lett. 32 (1978) 413.
[5] R. Fantoni, E. Borsella, S. Piccirillo, A. Giardini-Guidoni, R. Teghil, Laser Chem. 8 (1988) 385.
[6] Z. Li, J.S. Francisco, J. Chem. Phys. 96 (1992) 878.
[7] C.R. Quick Jr., C. Wittig, Chem. Phys. 32 (1978) 75.
[8] F.M. Lussier, J.J. Steinfeld, T.F. Deutsch, Chem. Phys. Lett. 58 (1978) 277.
[9] K. Saito, T. Yokubo, T. Fuse, H. Tahara, O. Kondo, T. Higashihara, Y. Murakami, Bull. Chem. Soc. Jpn. 52 (1979) 3507.
[10] A.M. Wodtke, E.J. Hintsa, J. Somorjai, Y.T. Lee, Isr. J. Chem. 29 (1989) 383.
[11] M. Oujja, J. Ruiz, R. de Nalda, M. Castillejo, Laser Chem. 16 (1996) 207.
[12] F.M. Lussier, J.I. Steinfeld, Chem. Phys. Lett. 50 (1977) 175.
[13] C.R. Quick Jr., C. Wittig, J. Chem. Phys. 69 (1978) 4201.
[14] M. Santos, L. Díaz, J.A. Torresano, J. Pola, J. Photochem. Photobiol. A: Chem. 104 (1997) 19.
[15] M. Castillejo, R. de Nalda, M. Oujja, L. Díaz, M. Santos, J. Photochem. Photobiol. A: Chem. 110 (1997) 107.
[16] H. Reisler, C. Wittig, In: J. Jortner, R.D. Levine, S.A. Rice (Eds.), Advances in Chemical Physics, Vol. 47, Wiley, New York, 1981, pp. 679–711.
[17] K.K. Pushpa, Awadhesh Kumar, R.K. Vatsa, P.D. Naik, K. Annaji Rao, J.P. Mittal, V. Parthasarathy, S.K. Sarkar, Chem. Phys. 240 (1985) 489.
[18] K.K. Pushpa, Awadhesh Kumar, P.D. Naik, K. Annaji Rao, V. Parthasarathy, S.K. Sarkar, J.P. Mittal, Chem. Phys. Lett. 279 (1997) 172.
[19] M.H. Yu, H. Reisler, M. Mangir, C. Wittig, Chem. Phys. Lett. 62 (1979) 439.
[20] M.T. Duignan, E. Grunwald, S. Spelser, J. Phys. Chem. 87 (1983) 4387.
[21] M.H. Yu, M.R. Levy, C. Wittig, J. Chem. Phys. 72 (1980) 3789.
[22] M.L. Lesiecki, W.A. Guillory, J. Chem. Phys. 66 (1977) 4317.
[23] J.C. Stephenson, D.S. King, M.F. Goodman, J. Stone, J. Chem. Phys. 70 (1979) 4496.
[24] D.C. Tardy, B.S. Rabinovitch, Chem. Rev. 77 (1977) 369.
[25] L.C.M. Miller, J.S. McKillop, N. Zare, J. Chem. Phys. 76 (1982) 2390.
[26] J.H. Hall Jr., M.L. Lesieck, W.A. Guillory, J. Chem. Phys. 68 (1978) 2247.
[27] L. Danylewych, R.W. Nicholls, Proc. R. Soc. Lond. A 339 (1974) 197.
[28] G. Stark, S.P. Davis, Z. Phys. A 321 (1985) 75.
[29] R.S. Urdahl, Y. Bao, W.M. Jackson, Chem. Phys. Lett. 152 (1988) 485.
[30] W. Bauer, K.H. Becker, M. Bielefeld, R. Meuser, Chem. Phys. Lett. 123 (1986) 33.
[31] M. Martin, J. Photochem. Photobiol. A: Chem. 66 (1992) 263.
[32] M. Castillejo, M. Martín, R. de Nalda, J. Solis, Chem. Phys. Lett. 268 (1997) 465.
[33] S.A. Abrash, R.W. Zehner, G.J. Mains, L.M. Raff, J. Phys. Chem. 99 (1995) 2959.
[34] R. Pan, L.M. Raff, J. Phys. Chem. 100 (1996) 8085.
[35] R.D. Kay, L.M. Raff, J. Phys. Chem. 101 (1997) 1007.
[36] G.J. Mains, L.M. Raff, S.M. Abrash, J. Phys. Chem. 99 (1995) 3532.
[37] S.P. Walch, P.R. Taylor, J. Chem. Phys. 103 (1995) 4975.